PNAS RESEARCH ARTICLE | MICROBIOLOGY

YfmR is a translation factor that prevents ribosome stalling and cell death in the absence of EF-P

Hye-Rim Hong[a], Cassidy R. Prince[a], Daniel D. Tetreault[a], Letian Wu[a], and Heather A. Feaga[a,1]

Edited by Daniel B. Kearns, Indiana University Bloomington, Bloomington, IN; received August 21, 2023; accepted January 9, 2024 by Editorial Board Member Tina M. Henkin

Protein synthesis is performed by the ribosome and a host of highly conserved elongation factors. Elongation factor P (EF-P) prevents ribosome stalling at difficult-to-translate sequences, such as polyproline tracts. In bacteria, phenotypes associated with *efp* deletion range from modest to lethal, suggesting that some species encode an additional translation factor that has similar function to EF-P. Here we identify YfmR as a translation factor that is essential in the absence of EF-P in *Bacillus subtilis*. YfmR is an ABCF ATPase that is closely related to both Uup and EttA, ABCFs that bind the ribosomal E-site and are conserved in more than 50% of bacterial genomes. We show that YfmR associates with actively translating ribosomes and that depleting YfmR from Δ*efp* cells causes severe ribosome stalling at a polyproline tract in vivo. YfmR depletion from Δ*efp* cells was lethal and caused reduced levels of actively translating ribosomes. Our results therefore identify YfmR as an important translation factor that is essential in *B. subtilis* in the absence of EF-P.

ribosome | translation | ABCF | EF-P | bacteria

Significance

Translation is one of the most ancient and energetically demanding processes that occurs in the cell. Ribosomes constitute more than 60% of the cellular mass in actively growing cells, and ribosomes are a major target of antimicrobials and chemotherapeutics. Here, we identify YfmR as a translation factor that is essential in the absence of EF-P. YfmR is a member of the ABCF family of ATPases whose role in translation is only beginning to be understood. Given the broad distribution of ABCFs from bacteria to fungi, we expect our results to have implications for understanding translation elongation in diverse organisms.

Ribosomes catalyze peptide bond formation by using a series of tRNAs to decode an mRNA template. In bacteria, translation initiates when an mRNA and the initiation factors IF1, IF2, and IF3 bind the small 30S ribosomal subunit (1). IF2 and IF3 ensure that a specialized tRNA charged with formyl-methionine ($tRNA^{fMet}$) is positioned at the P-site during initiation (2–6). After IF3 dissociates, the large 50S subunit joins to form the 70S initiation complex (70SIC) (7). IF1 and IF2 then dissociate, and charged tRNAs are delivered to the A-site of the 70S elongation complex (70SEC) by EF-Tu (8, 9). The large ribosomal subunit catalyzes peptide bond formation and the nascent chain is transferred from the P-site tRNA to the A-site tRNA (10–13). The ribosome is then advanced one codon by EF-G (14–16). Elongation proceeds at a rate of approximately 15 codons s^{-1} (17) and terminates at a stop codon.

Ribosomes become stalled at polyproline tracts because the cyclical nature of proline causes an unfavorable conformation of the nascent peptide in the exit tunnel that destabilizes the peptidyl-tRNA in the P-site (18). In bacteria, the near universally conserved elongation factor EF-P prevents ribosome stalling at prolines by stabilizing the P-site tRNA and forcing the nascent chain to adopt a favorable geometry for peptide bond formation (18–25). Structural and biochemical data also support a role for EF-P in promoting the formation of the first peptide bond (26–28). EF-P stimulates peptide bond formation in vitro between fMet-Lys, fMet-Leu, and fMet-Gly, though not between fMet-Phe (26, 29). Both $tRNA^{fMet}$ and $tRNA^{Pro}$ are unique in that they contain a C17pU17a bulge in the D-loop, which could serve as a specificity determinant for EF-P (18, 30–32).

EF-P is essential in some bacterial species, such as *Acinetobacter baumannii* (33), *Neisseria meningitidis* (34), and *Mycobacterium tuberculosis* (35), but is dispensable in others, such as *Salmonella enterica* (36), *Escherichia coli* (37–39), and *Bacillus subtilis* (37, 40–44). Since *efp* deletion phenotypes range from modest to lethal in different bacterial species, we hypothesized that some bacteria encode an uncharacterized translation factor with a similar function. To identify this factor, we used transposon mutagenesis coupled to Illumina sequencing (Tn-seq) to screen for genes that are essential in the absence of EF-P in *B. subtilis*. This screen identified *yfmR* as a gene that is essential when *efp* is deleted. We find that depleting YfmR from Δ*efp* cells causes severe ribosome stalling at a polyproline tract and decreases actively translating ribosomes. We also find that deleting *efp* from *Bacillus anthracis* causes severe growth and sporulation defects and that heterologous expression of *B. subtilis* YfmR in *B. anthracis* Δ*efp* cells partially rescues these phenotypes. These results suggest that YfmR and EF-P have similar functions in preventing ribosome stalling and that this function is essential in *B. subtilis*.

Author affiliations: [a]Department of Microbiology, Cornell University, Ithaca, NY 14853

Author contributions: H.-R.H., C.R.P., and H.A.F. designed research; H.-R.H., C.R.P., L.W., and H.A.F. performed research; H.-R.H., D.D.T., and H.A.F. contributed new reagents/analytic tools; H.-R.H., C.R.P., and H.A.F. analyzed data; and H.-R.H. and H.A.F. wrote the paper.

The authors declare no competing interest.

This article is a PNAS Direct Submission. D.B.K. is a guest editor invited by the Editorial Board.

[1]To whom correspondence may be addressed. Email: haf54@cornell.edu.

This article contains supporting information online at https://www.pnas.org/lookup/suppl/doi:10.1073/pnas.2314437121/-/DCSupplemental.

Published February 13, 2024.

Results

Tn-Seq Identifies Genetic Interactions with *efp*. EF-P is essential in some bacterial species but dispensable in others, suggesting that some species encode translation factors with compensatory or redundant functions. To identify genes that may be essential in the absence of EF-P in *B. subtilis*, we performed transposon mutagenesis followed by Illumina sequencing (Tn-seq). We transformed *B. subtilis* genomic DNA that had been transposon mutagenized in vitro (45) into wild-type or Δ*efp* cells (Fig. 1*A*). We pooled libraries of >450,000 colonies from each strain, then mapped and tallied the transposon insertion sites (Fig. 1*B*) (Dataset S1). Genes with few insertions in both wild-type and Δ*efp* cells are likely to be essential in both strains, whereas genes that have fewer insertions in Δ*efp* cells compared to wild-type are likely to be more essential in the Δ*efp* background.

Genes with a low number of insertions in Δ*efp* cells compared to wild-type included several tRNAs that decode codons at which ribosomes stall in the Δ*efp* background (21, 46). Two of the three $tRNA^{Pro}$ genes (*trnJ-Pro* and *trnI-Pro*) had greater than five times as many insertions in the wild-type background compared to the Δ*efp* background (Fig. 1*B*). The third $tRNA^{Pro}$ gene (*trnB-Pro*) had very few insertions in both the wild-type and Δ*efp* background. Decoding of glycine is also strongly impacted by EF-P (21, 38, 47) and *trnI-Gly*, *trnE-Gly*, and *trnB-Gly2* averaged more than four times as many insertions in the wild type than the Δ*efp* background (Fig. 1*B*). We did not note an apparent interaction between *efp* and other known ribosome quality control factors. *smpB*, *ssrA*, *rqcH*, *mutS2*, and *brfA* all had similarly high numbers of insertions in both the wild-type and Δ*efp* backgrounds (Dataset S1).

Deletion of the gene encoding the ABCF ATPase YfmR Is Synthetically Lethal with *efp* Deletion. One of the genes with the most significant difference in transposon insertions between the wild-type and Δ*efp* strains was *yfmR* (Fig. 1*B*), which encodes an ABCF ATPase (48–50). *B. subtilis* Δ*efp* cells exhibited a 10-fold reduction in insertions in *yfmR* compared to wild type, suggesting that *yfmR* may be essential when *efp* is absent. *B. subtilis* encodes 4 ABCF ATPases, but only *yfmR* appeared to be essential in the Δ*efp* background. *yfmM* and *ydiF* had >100 insertions in both wild-type and Δ*efp* backgrounds, and *ykpA* had >50 insertions in both backgrounds (Dataset S1).

To test whether *yfmR* is essential in Δ*efp* cells, we first measured transformation efficiency of Δ*yfmR::kan*^{R} genomic DNA into a Δ*efp* background. Δ*spoIIE::kan*^{R} genomic DNA (carrying a deletion of

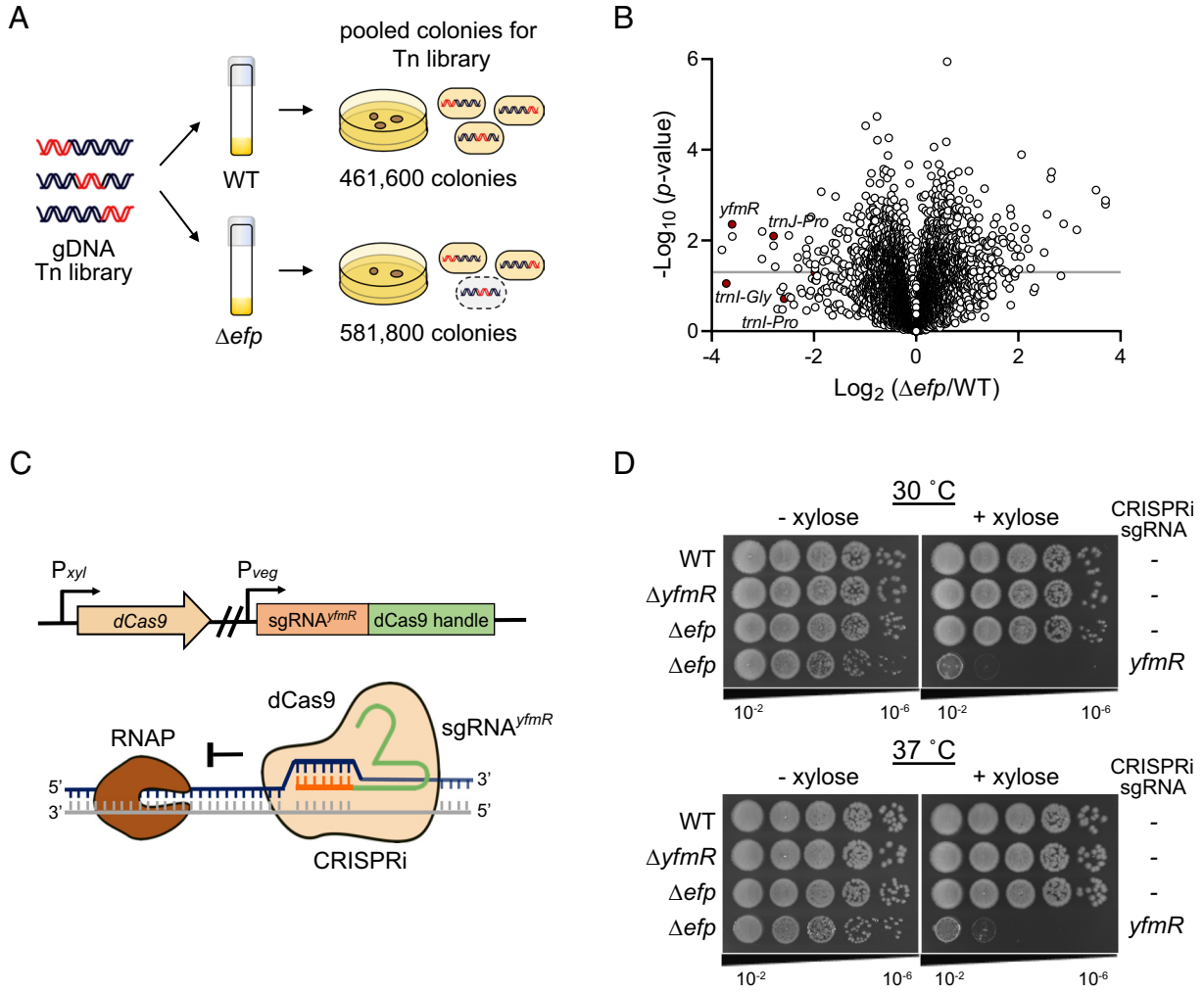

Fig. 1. YfmR depletion is lethal to *B. subtilis* in the absence of EF-P. (*A*) Schematic of transposon library generation. In vitro transposed *B. subtilis* genomic DNA was transformed into wild-type and Δ*efp* strains. Sequencing libraries were produced in triplicate. (*B*) Volcano plot showing the results of Tn-seq experiment. Gray bar indicates *P*-value of 0.05. (*C*) Schematic of CRISPR interference to deplete YfmR. Guide RNA targeting *yfmR* (sgRNA^{yfmR}) is constitutively expressed while deactivated Cas9 (dCas9) is expressed under the control of a xylose promoter. (*D*) *B. subtilis* Δ*efp* expressing dCas9+sgRNA^{yfmR} fails to form colonies at 30 °C and 37 °C. Log-phase cultures were serially diluted and then plated with and without xylose for induction of dCas9 to deplete YfmR. Spot plates are representative of four independent experiments.

the non-essential *spoIIE* gene) was used as a positive control. While the positive control plate had >1,000 colonies, only two colonies formed on the plate where *Δefp::mls* had been transformed with *ΔyfmR::kan*^{R}, and PCR revealed that both colonies maintained a wild-type copy of *yfmR* in addition to the *kan*^{R} allele, indicating the *kan*^{R} allele had inserted into a different locus.

Next, we used CRISPR interference (CRISPRi) (51, 52) to deplete YfmR from Δ*efp* (unmarked) cells by co-expressing nuclease deficient Cas9 (dCas9) and a guide RNA targeting *yfmR* (P_{xyl} – dCas9 P_{veg} – sgRNA^{yfmR}) (Fig. 1*C*). We will refer to this strain as Δ*efp* + YfmR^{depletion}. Single deletion of *yfmR* or *efp* did not significantly affect growth or colony size (Fig. 1*D*). However, when dCas9 with sgRNA^{yfmR} were co-expressed in Δ*efp* cells (Δ*efp* + YfmR^{depletion}), these cells failed to form colonies at both 30 °C and 37 °C (Fig. 1*D*), demonstrating that *yfmR* and *efp* are a synthetic lethal pair in *B. subtilis*.

YfmR Associates with 70S Ribosomes and Polysomes. To examine the association of YfmR with ribosomes, we expressed C-terminally Flag-tagged YfmR under the control of a $P_{hyperspank}$ promoter. We loaded cell lysate from this strain on a sucrose density gradient. After ultracentrifugation, we resolved an equal volume of each gradient fraction by SDS-PAGE and probed with an anti-Flag antibody. As a positive control for ribosome association, we probed these same fractions with a polyclonal antibody raised against *B. subtilis* EF-Tu (53). As a negative control for ribosome association, we expressed Flag-tagged RFPCFP under the control of a $P_{hyperspank}$ promoter and again probed sucrose density gradient fractions with the anti-Flag antibody. We detected YfmR associated with ribosomes, including in the polysome fractions, similar to EF-Tu (Fig. 2*A*). In contrast, the negative control protein, RFPCFP, was only detected at the top of the gradient as expected for a non-ribosome-associated protein. These data indicate that YfmR associates with actively translating ribosomes.

YfmR Depletion from Δ*efp* Cells Causes Severe Ribosome Stalling at a Polyproline Tract. EF-P binds to the ribosome between the E- and P-sites and assists translation of polyproline tracts and other difficult-to-translate sequences (18, 27). YfmR is closely related to Uup and EttA (50), ABCF ATPases that bind the ribosomal E-site and promote a favorable geometry for peptide bond formation (54). Therefore, we hypothesized that YfmR may play a role in rescuing ribosomes stalled at polyprolines and be functionally redundant with EF-P. To investigate this, we designed an N-terminally Flag-tagged reporter to quantify polyproline-induced stalling (Fig. 2*B*). An RFP-5Pro-CFP fusion was placed under the control of an IPTG-inducible promoter and integrated as a single copy into the chromosome of wild-type, Δ*efp* or Δ*efp* + YfmR^{depletion} backgrounds (Fig. 2*B*). A Flag-tagged protein of the same construction but lacking the polyproline motif was used as a control. Ribosome stalling at the polyproline tract results in a peptide that is approximately 30 kDa, whereas full-length protein is approximately 58 kDa. We report ribosome stalling as a percentage of stalled peptide divided by the total of both stalled plus full-length peptide. No ribosome stalling was detected in wild-type cells, whereas Δ*efp* cells exhibited severe ribosome stalling at the polyproline tract (37.42 ± 7.57% stalling). We did not detect ribosome stalling in the Δ*yfmR* single deletion (Fig. 2*B*). However, when YfmR was depleted from Δ*efp* cells ribosome stalling at the polyproline tract was significantly more severe than Δ*efp* deletion on its own (72.24 ± 2.9 % stalling in Δ*efp* + YfmR^{depletion})(P = 0.0018) (Fig. 2*B*). These data suggest

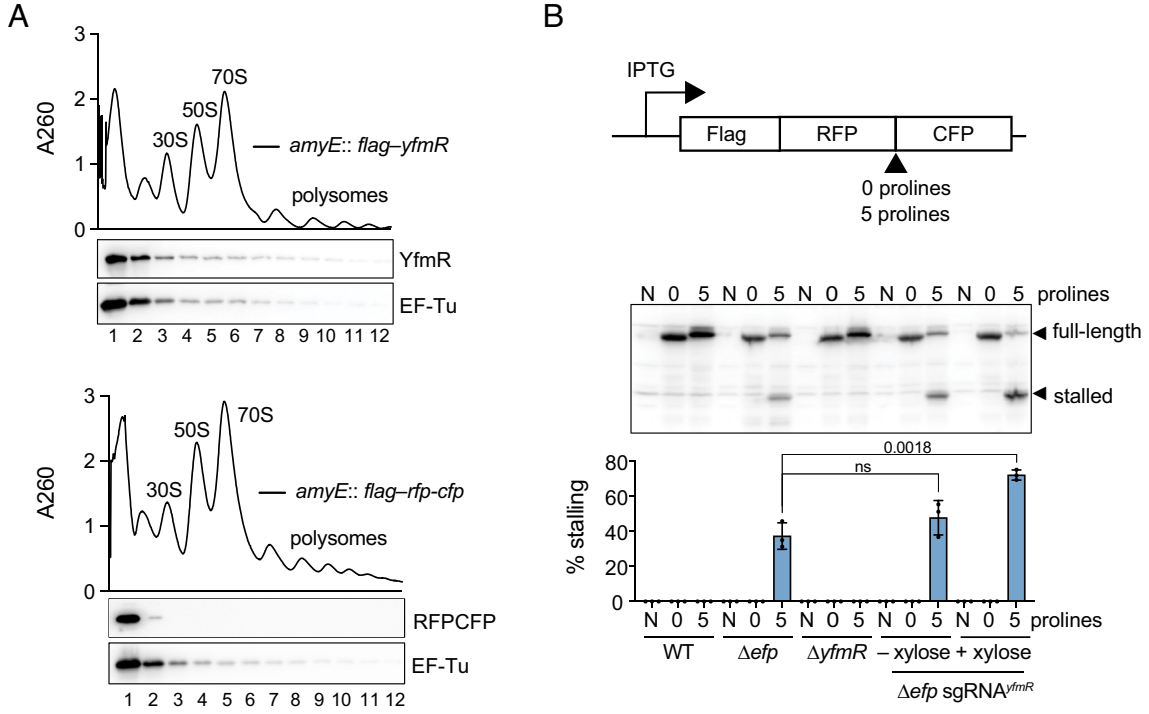

Fig. 2. YfmR associates with ribosomes and prevents ribosome stalling at a polyproline tract. (*A*) Strains expressing Flag-tagged YfmR (*Top*) or Flag-tagged RFPCFP (*Bottom*) were grown to late-log phase. Flag-tagged RFPCFP is shown as a negative control for ribosome association. Lysate from each strain was resolved by sucrose density gradient ultracentrifugation. Sucrose density gradient fractions for each strain were probed with anti-Flag antibody or with a polyclonal antibody raised against EF-Tu as a positive control for ribosome association. A260 traces and western blots are representative of three independent experiments. (*B*) Schematic of reporter for proline stalling and western blot showing full-length protein and truncated protein that results from ribosome stalling at the polyproline tract. Cell lysate was harvested after 3 h of simultaneous reporter expression and dCas9 induction to deplete YfmR. N indicates lysate from strain without reporter plasmid. 0 and 5 indicate reporters without a proline tract or with a proline tract containing five prolines. Error bars represent SD from three independent experiments. *P*-value indicates the results of an unpaired two-tailed *t* test.

that YfmR prevents ribosome stalling at a polyproline tract in the absence of EF-P.

Depleting YfmR from *Δefp* Cells Reduces Actively Translating Ribosomes and Increases Unengaged Ribosomal Subunits. To further investigate the impact of YfmR depletion in Δ*efp* cells, we used sucrose density gradient ultracentrifugation to characterize 30S and 50S ribosomal subunits, 70S ribosomes, and polysomes in wild-type, Δ*efp*, Δ*yfmR*, and Δ*efp* + YfmR^{depletion} cells. We quantified relative levels of each ribosome species by determining the area under the curve for each respective peak. Single deletions of *yfmR* or *efp* did not significantly impact levels of 30S, 50S, 70S or polysomes (Fig. 3*A* and *SI Appendix*, Fig. S1). In contrast, when YfmR was depleted from Δ*efp* cells, 70S ribosomes and polysomes decreased by 34.2 ± 6.1 % compared to wild type (Fig. 3*A*) (*SI Appendix*, Fig. S2) (P = 0.016). The significant decrease in 70S and polysomes indicates that there is a severe translation defect when YfmR is depleted from Δ*efp* cells.

Initiator tRNAs Are Enriched in 30S and 70S Ribosome Fractions in *Δefp* Cells When YfmR Is Depleted. Depleting YfmR from Δ*efp* cells resulted in decreased 70S ribosomes and polysomes and a relative increase in unengaged 30S and 50S subunits (Fig. 3*A*). To further explore defects in translation we assayed levels of initiator tRNA^{fMet}, tRNA^{Pro}, and tRNA^{Lys} associated with ribosomal subunits. We separated ribosomes by sucrose density gradient ultracentrifugation and precipitated total RNA from the 30S, 50S, 70S, and polysome peaks. The ratio of each tRNA relative to 16S rRNA was then quantified to determine levels of association with each ribosome species peak in wild-type, Δ*efp*, and Δ*efp* + YfmR^{depletion} backgrounds. Initiator tRNA^{fMet} association with the 30S and 70S peaks significantly increased when YfmR was depleted in Δ*efp* (P = 0.0031 and P = 0.02) (Fig. 3*B*). In contrast, levels of tRNA^{Pro} and tRNA^{Lys} associated with 30S or 70S did not increase in Δ*efp* cells when YfmR was depleted (Fig. 3*B* and *SI Appendix*, Fig. S2). Increased tRNA^{fMet} association with 30S ribosomes may indicate a failure of the 50S large subunit to join, whereas increased tRNA^{fMet} association with 70S ribosomes may indicate a failure in early elongation.

***E. coli* Uup Is Functionally Interchangeable with YfmR.** The *B. subtilis* YfmR structure predicted by AlphaFold (55) is similar to *E. coli* Uup and EttA (Fig. 4*A*)(30, 54). Bacterial ABCFs contain two ATPase domains separated by an approximately 80 amino acid linker called the P-site tRNA interacting motif (PtIM) (30, 56). ABCFs bind the ribosomal E-site, and their functional diversity may depend on the length and amino acid composition of the PtIM (54). EttA's PtIM domain (residues 242 to 322) makes specific contacts with tRNA^{fMet} (56) (Fig. 4*B*) and promotes a favorable geometry for peptide bond formation during elongation (30, 54, 56, 57). YfmR has comparable overall sequence identity to both EttA (36%) and Uup (35%) but is more similar to EttA in its PtIM (Fig. 4*C*). YfmR and Uup both have a coiled coil C-terminal extension that is absent in EttA (50, 58).

We compared ABCFs of *B. subtilis*, *B. anthracis*, and *E. coli* to examine their likely evolutionary history. Consistent with previous reports (50), we observed that EttA and Uup share a common ancestor exclusive of the other ABCFs with a maximum likelihood bootstrap percentage of >90% (Fig. 4*D*). YfmR from *B. subtilis* and from *B. anthracis* clustered with EttA instead of Uup, but with lower certainty (66% MLB).

To determine the functional relationship between Uup or EttA with YfmR, we then tested whether Uup or EttA from *E. coli* could rescue *B. subtilis* Δ*efp* when YfmR was depleted. We expressed either Uup or EttA from an IPTG-inducible promoter integrated into the chromosome of Δ*efp* P_{xyl}–dCas9 P_{veg}–sgRNA^{yfmR} (Δ*efp* + YfmR^{depletion}). Expression of Uup showed a complete rescue of Δ*efp* with YfmR depletion, whereas EttA did not (Fig. 4*E*). These data indicate that Uup is functionally interchangeable with YfmR in *B. subtilis*.

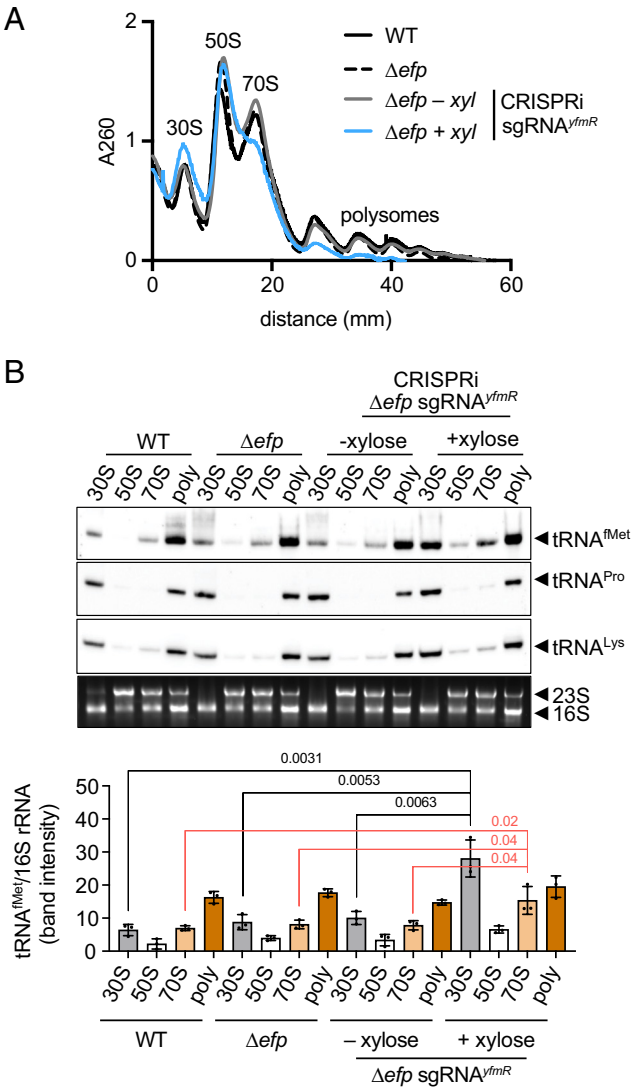

Fig. 3. Effect of YfmR depletion on ribosome activity and tRNA association in Δ*efp* cells. Cells were grown in LB at 37 °C with aeration and harvested at late-log phase. dCas9 was induced for 3 h to deplete YfmR. (*A*) Sucrose density gradient ribosome traces of wild type, Δ*efp*, and Δ*efp* with and without YfmR depletion. (*B*) Northern blot analysis of RNA precipitated from 30S, 50S, 70S, and polysome fractions using a probe specific to tRNA^{fMet}, tRNA^{Pro}, or tRNA^{Lys}. Error bars represent SD of three independent experiments. *P*-value indicates the results of an unpaired two-tailed *t* test. See *SI Appendix*, Fig. S2 for quantification of tRNA^{Pro} and tRNA^{Lys}.

***B. subtilis* YfmR Partially Rescues *B. anthracis* Δ*efp* Growth and Sporulation Defects.** An outstanding mystery in the field is why Δ*efp* phenotypes range from modest to lethal in bacteria (38). To investigate this, we determined the phenotype of Δ*efp* in *B. anthracis*, which encodes a similar number of polyproline tracts as *B. subtilis*. While single deletion of *efp* in *B. subtilis* does not significantly impact growth rate and only modestly impacts sporulation efficiency (37, 44), we observed that *B. anthracis* Δ*efp* exhibits severe growth defects at both 30 °C and 37 °C, produces no detectable spores, and exhibits ribosome stalling at a polyproline tract (Fig. 5 *A* and *B* and *SI Appendix*, Fig. S3).

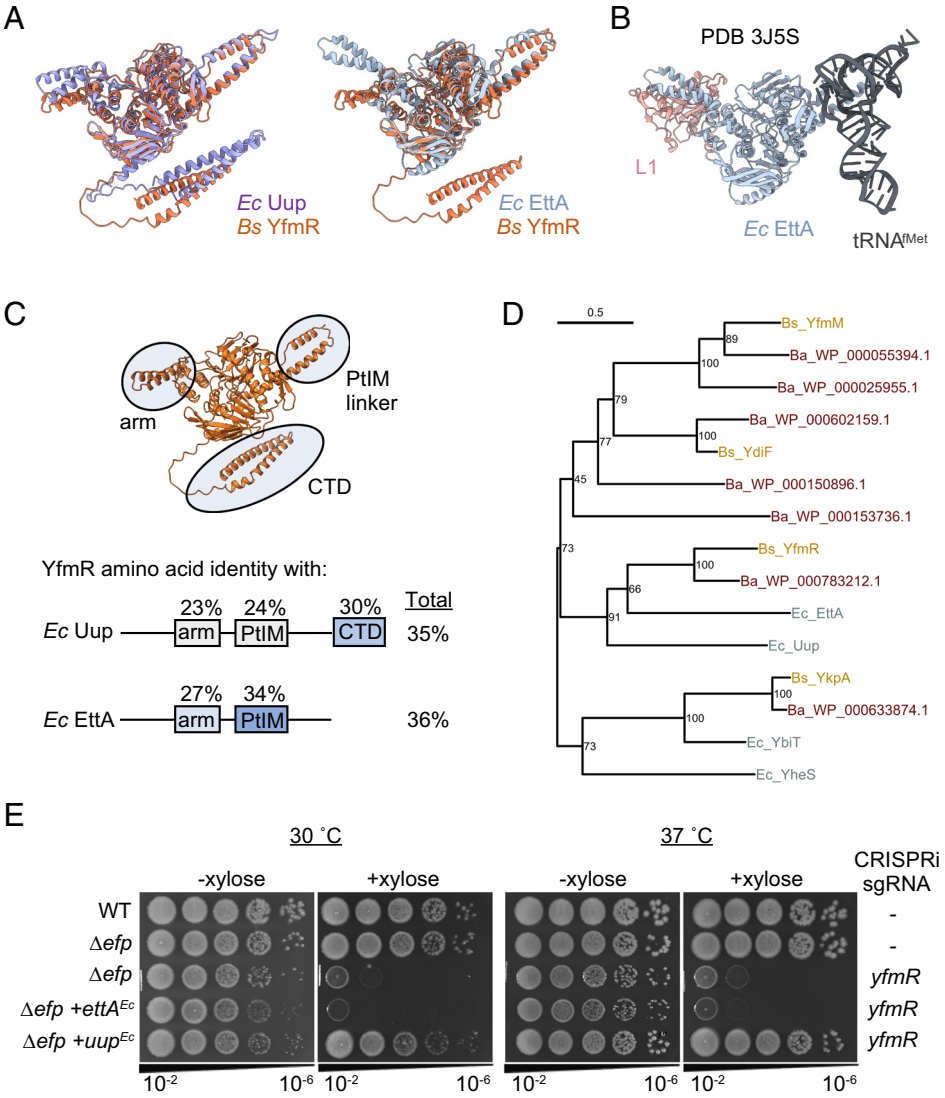

Fig. 4. Structural, phylogenetic, and functional relationships between YfmR, Uup, and EttA. (*A*) AlphaFold predicted structures of *B. subtilis* YfmR overlayed with *E. coli* Uup or EttA. (*B*) Structure of *E. coli* EttA with ribosomal protein L1 and tRNA^{fMet} (PDB 3J5S). (*C*) Domain homology analysis comparing YfmR to Uup and EttA. Arm domain includes YfmR residues 91 to 147. PtIM domain includes YfmR residues 239 to 318. C-terminal domain includes YfmR residues 539 to 629. (*D*) Phylogenetic tree of amino acid sequences of ABCFs from *B. subtilis*, *B. anthracis,* and *E. coli*. Numbers at nodes indicate maximum likelihood bootstrap percentage, which indicates likelihood of a common ancestor between the two branches. (*E*) Spot plates with and without YfmR depletion in Δ*efp* or Δ*efp* expressing either Uup or EttA from *E. coli*.

Notably, similar translation defects occur in *B. anthracis* Δ*efp* single deletion as occur in *B. subtilis* Δ*efp* when YfmR is depleted (*SI Appendix*, Fig. S4 *A* and *B*).

To test whether *B. subtilis* YfmR could complement the *B. anthracis* growth defect, we expressed IPTG-inducible YfmR from *B. subtilis* as a single copy integrated into the *B. anthracis* genome (Fig. 5*A*). Expression of *B. subtilis* YfmR partially but significantly rescued the growth defect of *B. anthracis* Δ*efp* at both 30 °C (P = 0.04) and 37 °C (P = 0.01). Expression of *B. subtilis* YfmR also partially rescued the *B. anthracis* Δ*efp* sporulation defect (Fig. 5*B*).

B. anthracis encodes a YfmR homolog (WP_000783212.1) that shares 57% amino acid sequence identity with *B. subtilis* YfmR. Structural modeling with AlphaFold (55) of *B. subtilis* and *B. anthracis* YfmR shows that they are structurally similar (*SI Appendix*, Fig. S5). To determine whether *B. anthracis* YfmR is functional, we tested whether it could rescue depletion of YfmR in *B. subtilis* Δ*efp*. Expressing *B. anthracis* YfmR from an IPTG-inducible promoter in *B. subtilis* Δ*efp* + YfmR^{depletion} restored colony formation to wild type levels (Fig. 5*C*). These data suggest that *B. anthracis* YfmR is active and functionally redundant with *B. subtilis* YfmR. Therefore, the presence or absence of an ABCF ATPase may not be sufficient to explain the variability in phenotypes of Δ*efp* mutants, and expression levels of the ABCFs must also be considered.

Discussion

Here, we identify YfmR as a translation factor that is essential in the absence of EF-P in *B. subtilis* (Fig. 1). We confirmed the essentiality of *yfmR* in Δ*efp* cells by CRISPRi (Fig. 1). YfmR associates with *B. subtilis* ribosomes, including polysomes (Fig. 2). YfmR depletion from Δ*efp* cells causes severe ribosome stalling at a poly-proline tract and reduces levels of actively translating ribosomes (Figs. 2 and 3). These data support a role for YfmR in translation elongation and prevention of ribosome stalling. Additionally, we report that *B. anthracis* Δ*efp* exhibits severe growth and sporulation defects, which can be partially rescued by YfmR from *B. subtilis*, further highlighting the importance of YfmR and its functional redundancy with EF-P (Fig. 5).

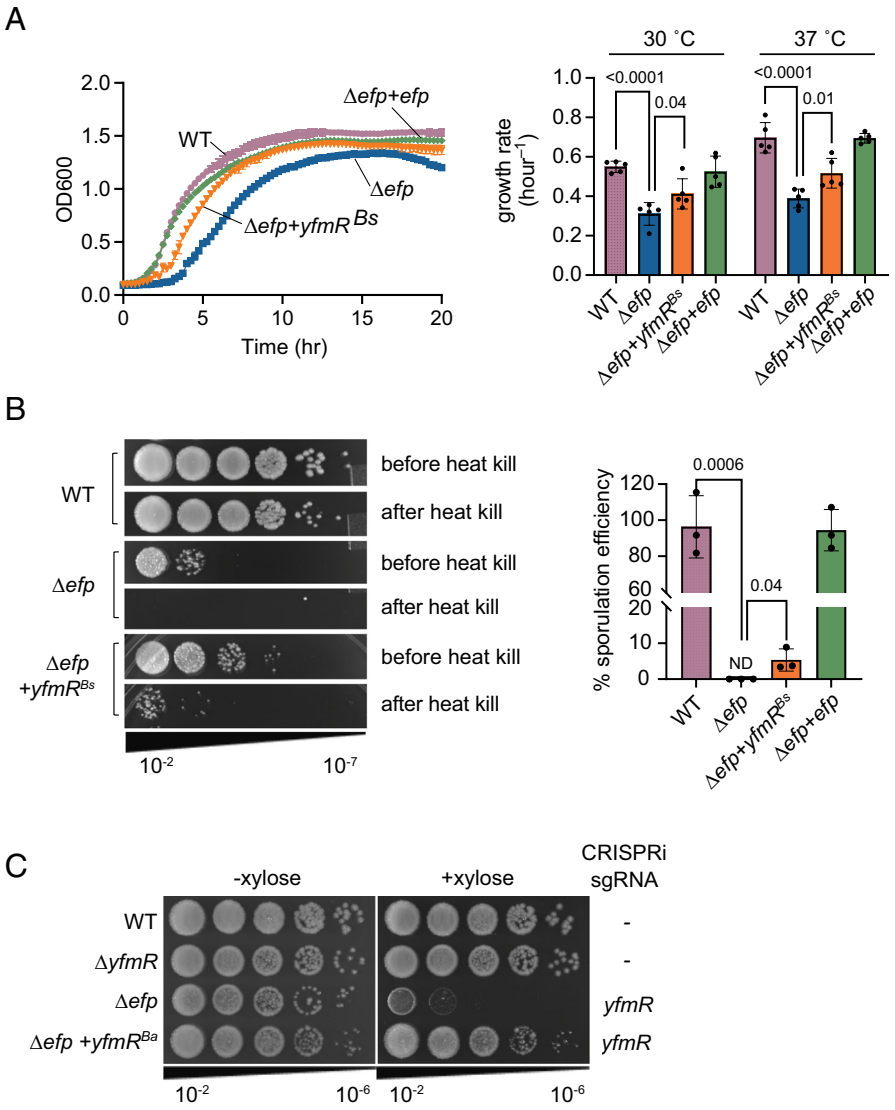

Fig. 5. Heterologous expression of *B. subtilis* YfmR in *B. anthracis* Δ*efp* partially rescues growth and sporulation defects. A single copy of *yfmR* from *B. subtilis* (*yfmR*^{Bs}) was integrated into the *B. anthracis* chromosome under the control of an IPTG-inducible promoter. (*A*) Growth curves of *B. anthracis* wild type, Δ*efp* and Δ*efp* expressing *B. subtilis yfmR*. Growth rates were determined at early log-phase. Error bars represent SD of five biological replicates. *P*-value indicates the results of an unpaired two-tailed *t* test. (*B*) *B. anthracis* wild type, Δ*efp,* and Δ*efp* expressing *B. subtilis yfmR* were sporulated for 24 h in DSM. Culture was serially diluted and plated before and after heating to 80 °C for 20 min to kill non-sporulated cells. Error bars represent SD of three biological replicates. *P*-values were determined by an unpaired two-tailed *t* test. (*C*) Spot plates showing that a single copy of *B. anthracis yfmR* (*yfmR*^{Ba}) integrated into the *B. subtilis* chromosome rescues depletion of the native YfmR from *B. subtilis* Δ*efp*.

Depleting YfmR from Δ*efp* cells caused more severe ribosome stalling at a polyproline tract than *efp* deletion on its own (Fig. 2*B*), suggesting that YfmR and EF-P have redundant functions in preventing ribosome stalling at polyprolines. Ribosome stalling at polyproline tracts in essential genes could explain the synthetic lethal phenotype of Δ*efp* Δ*yfmR*. Essential or quasi-essential genes containing a polyproline motif in *B. subtilis* include *topA*, *fmt*, and *valS*, which encode DNA topoisomerase I, methionyl-tRNA formyltransferase (FMT), and valine tRNA synthetase (ValS), respectively (59–62). FMT is of particular interest in the context of our results because it adds the N-formyl group to Met-tRNA^{fMet}, which helps it to be recognized by IF2 and to resist peptidyl-tRNA hydrolysis (63, 64). The ValS tRNA synthetase is also of interest since it contains a polyproline motif that is highly conserved across eukaryotic, archaeal, and bacterial proteomes (65). It has been proposed that EF-P is universally conserved, in part, to efficiently translate this protein (65, 66).

YfmR associates with 70S ribosomes and polysomes, suggesting that it plays a role in translation elongation (Fig. 2*A*). Reduced 70S ribosomes and polysomes and the specific enrichment of tRNA^{fMet} associated with 30S and 70S subunits in Δ*efp* + YfmR^{depletion} further suggest that there is a failure in translation initiation or early elongation in the absence of EF-P and YfmR (Fig. 3). EF-P can promote early elongation at some amino acids in vitro (26, 28). Therefore, further experiments are required to determine whether YfmR can also facilitate early elongation or whether the decreased translation we observe is an indirect result of cell death or the failure to produce an essential translation factor containing a polyproline motif.

YfmR is closely related to both Uup and EttA (Fig. 4) (50). Heterologous expression of *E. coli* Uup restored growth of *B. subtilis* Δ*efp* cells when YfmR was depleted (Fig. 4*E*), suggesting that YfmR and Uup have a similar function in vivo. Uup does not stimulate peptide bond formation in a tripeptide assay using fMet-Phe-Lys (57). However, it is possible that, like EF-P, Uup does not stimulate peptide bond formation between fMet-Phe but may stimulate peptide bond formation between fMet and other amino acids (26, 29). Indeed, a recent preprint showed that Uup increased production of a peptide encoding a polyproline tract

in vitro (67). Moreover, Uup-EQ2 has similar binding affinity for both initiating and elongating ribosomes (54), further suggesting that Uup may function in elongation. Uup also likely plays a role in ribosome biogenesis since Δ*bipA* Δ*uup* cells accumulate immature 50S subunits (50, 68). Since EF-P does not play a role in ribosome biogenesis, our data suggest that the essential function of YfmR/Uup in the absence of EF-P is not ribosome biogenesis, but prevention of ribosome stalling.

ABCFs are near-universally conserved in bacterial genomes, with an average of four paralogs encoded per genome (50). The diverse functions of these highly conserved proteins are just beginning to be determined. Many important questions remain regarding their evolution, functional overlap, regulation, and mechanisms of action. Our work reveals the physiological importance of one of the most highly conserved ABCFs (YfmR/Uup) in maintaining cell viability and preventing ribosome stalling in vivo.

Methods

See *SI Appendix*, *Materials and Methods* for detailed descriptions. Strains, plasmids, and primers are found in *SI Appendix*, Tables S1–S3.

Strains and Media. All strains were derived from *B. subtilis* 168 *trpC2* and *B. anthracis* Sterne 34F2. *B. subtilis* and *B. anthracis* were grown in LB media at 30 °C and 37 °C as indicated. Sporulation was induced in Difco Sporulation Media (DSM) with aeration for 24 h at 37 °C.

Strain Construction. Markerless *efp* deletion in *B. anthracis* was made by two-step recombination as previously described (69). Gene deletions in *B. subtilis* were made by transforming genomic DNA from a BKK strain deletion into wild-type *B. subtilis 168 trpC2* (HAF1) (59). Δ*efp* + YfmR^{depletion} was constructed by expressing dCas9 under the control of a xylose-inducible promoter (51) while expressing a guide RNA targeting *yfmR* from a vegetative promoter in the Δ*efp* markerless background.

Tn-Seq Library and Sequencing. Magellan6x in vitro transposed gDNA prepared from wild-type *B. subtilis* 168 (45) was transformed into wild-type or Δ*efp B. subtilis*. Transposon insertions were sequenced on the Illumina MiSeq platform (v3 150 bp kit) at the Cornell University Biotechnology Resource Center.

Measuring Proline Stalling. $P_{hyperspank}$–3xFLAG–RFP–linker–CFP was integrated at *thrC* in the wild-type, Δ*efp*, or Δ*efp* + YfmR^{depletion} background. The linker contained 0 or 5 prolines. The proline staller was induced with 1 mM IPTG at the same time the sgRNA^{yfmR} was induced with 5% xylose. Induction of the reporter and depletion of YfmR proceeded for 3 h before harvesting cells.

Sucrose Gradient Fractionation. Wild-type, Δ*efp* or Δ*efp* + YfmR^{depletion} cells were grown in LB starting from an OD of 0.05. Xylose was added to 5% to induce dCas9 and cells were harvested 3 h later. Clarified cell lysates were normalized to 1,500 ng/μL and loaded onto 10 to 40% sucrose gradients.

Northern Blotting and RNA Gels. RNA from sucrose gradient fractions were precipitated and normalized to 1 μg RNA. RNA was resolved on a TBE-Urea gel and transferred to a positively charged nylon membrane. RNA was probed with a biotinylated oligo specific for tRNA^{fMet}, tRNA^{Pro}, or tRNA^{Lys}. Oligo sequences are in *SI Appendix*, Table S3.

Structure Modeling and Sequence Comparison of ABCFs. The *E. coli* EttA structure was obtained from Protein Data Bank (PDB 3J5S) (30). YfmR structures for *B. subtilis* and *B. anthracis* were generated with AlphaFold (55). Molecular graphics and analysis were performed with ChimeraX v1.5 (70). ABCF protein sequences were downloaded from NCBI *E. coli* str. K–12 substr. MG1655 (NC_000913.3) and *B. subtilis* subsp. subtilis str. 168 (NC_000964.3) reference genomes as annotated by the NCBI Prokaryotic Genome Annotation Pipeline (71).

Data, Materials, and Software Availability. Sequencing data are available at Gene Expression Omnibus accession GSE249203 (72). An excel table containing the results of the Tn-seq can be found in *SI Appendix* (Dataset S1). Strains and plasmids are available upon request.

ACKNOWLEDGMENTS. We are grateful to lab members Katrina Callan and Kevin England for feedback and discussion of the work. We are grateful to Scott Stibitz and Roger Plaut for sharing pRP1099, pRP1028, pSS1827 and for advice on constructing gene deletions in *B. anthracis* Sterne. We are grateful to Christopher Johnson and Alan Grossman for sharing their transposon library. H.A.F., H.-R.H., L.W., D.D.T., and C.R.P. were supported by NIH grant R35GM147049. L.W. was supported by an undergraduate research fellowship from the Cornell Institute of Host-Microbe Interactions and Disease.

1. T. M. Schmeing, V. Ramakrishnan, What recent ribosome structures have revealed about the mechanism of translation. *Nature* **461**, 1234–1242 (2009).
2. M. Guenneugues *et al.*, Mapping the fMet-tRNA(f)(Met) binding site of initiation factor IF2. *Embo J* **19**, 5233–5240 (2000).
3. A. Simonetti *et al.*, Structure of the 30S translation initiation complex. *Nature* **455**, 416–420 (2008).
4. T. Hussain, J. L. Llácer, B. T. Wimberly, J. S. Kieft, V. Ramakrishnan, Large-scale movements of IF3 and tRNA during bacterial translation initiation. *Cell* **167**, 133–144.e113 (2016).
5. S. Kaledhonkar *et al.*, Late steps in bacterial translation initiation visualized using time-resolved cryo-EM. *Nature* **570**, 400–404 (2019).
6. K. Caban, M. Pavlov, M. Ehrenberg, R. L. Gonzalez Jr., A conformational switch in initiation factor 2 controls the fidelity of translation initiation in bacteria. *Nat. Commun.* **8**, 1475 (2017).
7. A. Simonetti *et al.*, Involvement of protein IF2 N domain in ribosomal subunit joining revealed from architecture and function of the full-length initiation factor. *Proc. Natl. Acad. Sci. U.S.A.* **110**, 15656–15661 (2013).
8. T. Pape, W. Wintermeyer, M. V. Rodnina, Complete kinetic mechanism of elongation factor Tu-dependent binding of aminoacyl-tRNA to the A site of the *E. coli* ribosome. *Embo J.* **17**, 7490–7497 (1998).
9. J. Czworkowski, P. B. Moore, The elongation phase of protein synthesis. *Prog. Nucleic Acid Res. Mol. Biol.* **54**, 293–332 (1996).
10. P. Nissen, J. Hansen, N. Ban, P. B. Moore, T. A. Steitz, The structural basis of ribosome activity in peptide bond synthesis. *Science* **289**, 920–930 (2000).
11. M. Simonović, T. A. Steitz, A structural view on the mechanism of the ribosome-catalyzed peptide bond formation. *Biochim. Biophys. Acta* **1789**, 612–623 (2009).
12. S. Kuhlenkoetter, W. Wintermeyer, M. V. Rodnina, Different substrate-dependent transition states in the active site of the ribosome. *Nature* **476**, 351–354 (2011).
13. M. Selmer *et al.*, Structure of the 70S ribosome complexed with mRNA and tRNA. *Science* **313**, 1935–1942 (2006).
14. D. Moazed, H. F. Noller, Intermediate states in the movement of transfer RNA in the ribosome. *Nature* **342**, 142–148 (1989).
15. M. V. Rodnina, A. Savelsbergh, V. I. Katunin, W. Wintermeyer, Hydrolysis of GTP by elongation factor G drives tRNA movement on the ribosome. *Nature* **385**, 37–41 (1997).
16. Y. G. Gao *et al.*, The structure of the ribosome with elongation factor G trapped in the posttranslocational state. *Science* **326**, 694–699 (2009).
17. G. E. Johnson, J. B. Lalanne, M. L. Peters, G. W. Li, Functionally uncoupled transcription-translation in Bacillus subtilis. *Nature* **585**, 124–128 (2020).
18. P. Huter *et al.*, Structural basis for polyproline-mediated ribosome stalling and rescue by the translation elongation factor EF-P. *Mol. Cell* **68**, 515–527.e516 (2017).
19. B. R. Glick, M. C. Ganoza, Identification of a soluble protein that stimulates peptide bond synthesis. *Proc. Natl. Acad. Sci. U.S.A.* **72**, 4257–4260 (1975).
20. S. Ude *et al.*, Translation elongation factor EF-P alleviates ribosome stalling at polyproline stretches. *Science* **339**, 82–85 (2013).
21. L. Peil *et al.*, Distinct XPPX sequence motifs induce ribosome stalling, which is rescued by the translation elongation factor EF-P. *Proc. Natl. Acad. Sci. U.S.A.* **110**, 15265–15270 (2013).
22. C. J. Woolstenhulme *et al.*, Nascent peptides that block protein synthesis in bacteria. *Proc. Natl. Acad. Sci. U.S.A.* **110**, E878–887 (2013).
23. L. K. Doerfel *et al.*, Entropic contribution of elongation factor P to proline positioning at the catalytic center of the ribosome. *J. Am. Chem. Soc.* **137**, 12997–13006 (2015).
24. K. R. Hummels, D. B. Kearns, Translation elongation factor P (EF-P). *FEMS Microbiol. Rev.* **44**, 208–218 (2020).
25. C. J. Woolstenhulme, N. R. Guydosh, R. Green, A. R. Buskirk, High-precision analysis of translational pausing by ribosome profiling in bacteria lacking EFP. *Cell Rep.* **11**, 13–21 (2015).
26. B. R. Glick, S. Chládek, M. C. Ganoza, Peptide bond formation stimulated by protein synthesis factor EF-P depends on the aminoacyl moiety of the acceptor. *Eur. J. Biochem.* **97**, 23–28 (1979).
27. G. Blaha, R. E. Stanley, T. A. Steitz, Formation of the first peptide bond: The structure of EF-P bound to the 70S ribosome. *Science* **325**, 966–970 (2009).
28. H. B. Gamper, I. Masuda, M. Frenkel-Morgenstern, Y. M. Hou, Maintenance of protein synthesis reading frame by EF-P and m(1)G37-tRNA. *Nat. Commun.* **6**, 7226 (2015).
29. T. J. Bullwinkle *et al.*, R)-β-lysine-modified elongation factor P functions in translation elongation. *J. Biol. Chem.* **288**, 4416–4423 (2013).
30. B. Chen *et al.*, EttA regulates translation by binding the ribosomal E site and restricting ribosome-tRNA dynamics. *Nat. Struct. Mol. Biol.* **21**, 152–159 (2014).
31. T. Katoh, I. Wohlgemuth, M. Nagano, M. V. Rodnina, H. Suga, Essential structural elements in tRNA(Pro) for EF-P–mediated alleviation of translation stalling. *Nat. Commun.* **7**, 11657 (2016).
32. F. Ousalem *et al.*, Global regulation via modulation of ribosome pausing by EttA. bioRxiv [Preprint] (2023). https://doi.org/10.1101/2023.10.17.562674 (Accessed 17 October 2023).
33. Q. Guo *et al.*, Elongation factor P modulates Acinetobacter baumannii physiology and virulence as a cyclic dimeric guanosine monophosphate effector. *Proc. Natl. Acad. Sci. U.S.A.* **119**, e2209838119 (2022).
34. T. Yanagisawa *et al.*, Neisseria meningitidis translation elongation factor P and its active-site arginine residue are essential for cell viability. *PLoS One* **11**, e0147907 (2016).

35. M. A. DeJesus *et al.*, Comprehensive essentiality analysis of the Mycobacterium tuberculosis genome via saturating transposon Mutagenesis. *mBio* **8**, e02133-16 (2017).
36. S. B. Zou *et al.*, Loss of elongation factor P disrupts bacterial outer membrane integrity. *J. Bacteriol.* **194**, 413–425 (2012).
37. R. Tollerson II, A. Witzky, M. Ibba, Elongation factor P is required to maintain proteome homeostasis at high growth rate. *Proc. Natl. Acad. Sci. U.S.A.* **115**, 11072–11077 (2018).
38. S. J. Hersch *et al.*, Divergent protein motifs direct elongation factor P-mediated translational regulation in Salmonella enterica and Escherichia coli. *mBio* **4**, e00180-00113 (2013).
39. C. J. Balibar, D. Iwanowicz, C. R. Dean, Elongation factor P is dispensable in Escherichia coli and Pseudomonas aeruginosa. *Curr. Microbiol.* **67**, 293–299 (2013).
40. D. B. Kearns, F. Chu, R. Rudner, R. Losick, Genes governing swarming in Bacillus subtilis and evidence for a phase variation mechanism controlling surface motility. *Mol. Microbiol.* **52**, 357–369 (2004).
41. A. Rajkovic *et al.*, Translation control of swarming proficiency in Bacillus subtilis by 5-amino-pentanolylated elongation factor p. *J. Biol. Chem.* **291**, 10976–10985 (2016).
42. A. Witzky *et al.*, EF-P posttranslational modification has variable impact on polyproline translation in Bacillus subtilis. *mBio* **9**, e00306-18 (2018).
43. K. R. Hummels, D. B. Kearns, Suppressor mutations in ribosomal proteins and FliY restore Bacillus subtilis swarming motility in the absence of EF-P. *PLoS Genet.* **15**, e1008179 (2019).
44. H. A. Feaga *et al.*, Elongation factor P is important for sporulation initiation. *J. Bacteriol.* **205**, e0037022 (2023).
45. C. M. Johnson, A. D. Grossman, Identification of host genes that affect acquisition of an integrative and conjugative element in Bacillus subtilis. *Mol. Microbiol.* **93**, 1284–1301 (2014).
46. E. D. Hoffer *et al.*, Structural insights into mRNA reading frame regulation by tRNA modification and slippery codon-anticodon pairing. *Elife* **9**, e51898 (2020).
47. L. K. Doerfel *et al.*, EF-P is essential for rapid synthesis of proteins containing consecutive proline residues. *Science* **339**, 85–88 (2013).
48. A. L. Davidson, E. Dassa, C. Orelle, J. Chen, Structure, function, and evolution of bacterial ATP-binding cassette systems. *Microbiol. Mol. Biol. Rev.* **72**, 317–364, table of contents (2008).
49. I. D. Kerr, Sequence analysis of twin ATP binding cassette proteins involved in translational control, antibiotic resistance, and ribonuclease L inhibition. *Biochem. Biophys. Res. Commun.* **315**, 166–173 (2004).
50. V. Murina *et al.*, ABCF ATPases involved in protein synthesis, ribosome assembly and antibiotic resistance: Structural and functional diversification across the tree of life. *J. Mol. Biol.* **431**, 3568–3590 (2019).
51. J. M. Peters *et al.*, A comprehensive, CRISPR-based functional analysis of essential genes in bacteria. *Cell* **165**, 1493–1506 (2016).
52. L. S. Qi *et al.*, Repurposing CRISPR as an RNA-guided platform for sequence-specific control of gene expression. *Cell* **152**, 1173–1183 (2013).
53. S. F. Pereira, R. L. Gonzalez Jr., J. Dworkin, Protein synthesis during cellular quiescence is inhibited by phosphorylation of a translational elongation factor. *Proc. Natl. Acad. Sci. U.S.A.* **112**, E3274–E3281 (2015).
54. S. Singh *et al.*, Cryo-EM studies of the four E. coli paralogs establish ABCF proteins as master plumbers of the peptidyl-transferase center of the ribosome. bioRxiv [Preprint] (2023). https://doi.org/10.1101/2023.06.15.543498 (Accessed 17 June 2023).
55. J. Jumper *et al.*, Highly accurate protein structure prediction with AlphaFold. *Nature* **596**, 583–589 (2021).
56. G. Boël *et al.*, The ABC-F protein EttA gates ribosome entry into the translation elongation cycle. *Nat. Struct. Mol. Biol.* **21**, 143–151 (2014).
57. F. Ousalem *et al.*, Comparative genetic, biochemical, and biophysical analyses of the four E. coli ABCF paralogs support distinct functions related to mRNA translation. bioRxiv [Preprint] (2023), https://doi.org/10.1101/2023.06.11.543863 (Accessed 12 June 2023).
58. L. Carlier, A. S. Haase, M. Y. Burgos Zepeda, E. Dassa, O. Lequin, The C-terminal domain of the Uup protein is a DNA-binding coiled coil motif. *J. Struct. Biol.* **180**, 577–584 (2012).
59. B. M. Koo *et al.*, Construction and analysis of two genome-scale deletion libraries for Bacillus subtilis. *Cell Syst.* **4**, 291–305.e297 (2017).
60. Y. Cai, P. Chandrangsu, A. Gaballa, J. D. Helmann, Lack of formylated methionyl-tRNA has pleiotropic effects on Bacillus subtilis. *Microbiology (Reading)* **163**, 185–196 (2017).
61. K. Kobayashi *et al.*, Essential Bacillus subtilis genes. *Proc. Natl. Acad. Sci. U.S.A.* **100**, 4678–4683 (2003).
62. H. B. Thomaides *et al.*, Essential bacterial functions encoded by gene pairs. *J. Bacteriol.* **189**, 591–602 (2007).
63. J. M. Guillon, Y. Mechulam, J. M. Schmitter, S. Blanquet, G. Fayat, Disruption of the gene for Met-tRNA(fMet) formyltransferase severely impairs growth of Escherichia coli. *J. Bacteriol.* **174**, 4294–4301 (1992).
64. L. H. Schulman, H. Pelka, The structural basis for the resistance of Escherichia coli formylmethionyl transfer ribonucleic acid to cleavage by Escherichia coli peptidyl transfer ribonucleic acid hydrolase. *J. Biol. Chem.* **250**, 542–547 (1975).
65. A. L. Starosta *et al.*, A conserved proline triplet in Val-tRNA synthetase and the origin of elongation factor P. *Cell Rep.* **9**, 476–483 (2014).
66. T. E. Brewer, A. Wagner, Horizontal gene transfer of a key translation protein has shaped the polyproline proteome. bioRxiv [Preprint] (2023). https://doi.org/10.1101/2023.10.19.563058 (Accessed 22 October 2023).
67. Y. Chadani, E. Uemura, K. Yamazaki, M. Kurihara, H. Taguchi, The ABCF proteins in Escherichia coli individually alleviate nascent peptide-induced noncanonical translations. bioRxiv [Preprint] (2023). https://doi.org/10.1101/2023.10.04.560807 (Accessed 5 October 2023).
68. K. L. Cochrane, "Elucidating ribosomes-genetic studies of the ATPase Uup and the ribosomal protein L1", Dissertation Thesis, University of Michigan (2015).
69. R. D. Plaut, S. Stibitz, Improvements to a markerless allelic exchange system for Bacillus anthracis. *PLoS One* **10**, e0142758 (2015).
70. E. F. Pettersen *et al.*, UCSF ChimeraX: Structure visualization for researchers, educators, and developers. *Protein Sci.* **30**, 70–82 (2021).
71. W. Li *et al.*, RefSeq: Expanding the prokaryotic genome annotation pipeline reach with protein family model curation. *Nucleic Acids Res.* **49**, D1020–D1028 (2021).
72. H. R. Hong, H. A. Feaga, YfmR is a translation factor that prevents ribosome stalling and cell death in the absence of EF-P. Gene Expression Omnibus. https://www.ncbi.nlm.nih.gov/geo/query/acc.cgi?acc=GSE249203. Deposited 1 December 2023.